Automotive Experiences
Vol. 6 No. 3 (2023) pp. 584-598
p-ISSN: 2615-6202 e-ISSN: 2615-6636

Research Paper

Theoretical Experiments on Road Profile Data Analysis using Filter Combinations

Djoko Wahyu Karmiadji[1,2], **M. Rosyidi**[3], **Tri Widodo**[4], **Harris Zenal**[1], **Nofriyadi Nurdam**[3], **Andi M. Kadir**[1], **Sofwan Hidayat**[4], **Sahid Bismantoko**[3], **Nurhadi Pramana**[3], **Winarno**[3]

[1]Research Center for Strength Structures Technology, National Research and Innovation, Indonesia
[2]Department of Mechanical Engineering, Pancasila University, Jakarta 12640, Indonesia
[3]Computation Research Center, National Research and Innovation, Indonesia
[4]Research Center for Transportation Technology, National Research and Innovation, Indonesia

djok001@brin.go.id

https://doi.org/10.31603/ae.9901

Published by Automotive Laboratory of Universitas Muhammadiyah Magelang collaboration with Association of Indonesian Vocational Educators (AIVE)

Article Info
Submitted:
14/08/2023
Revised:
12/09/2023
Accepted:
13/10/2023
Online first:
24/11/2023

Abstract

Identification of road profiles is needed to provide the input of automotive simulation and endurance testing. The analysis with estimation methods is mostly done to identify road profiles. The main goal of analysis methods is to obtain the data of vertical displacements due to road profile measurement. The acceleration data is obtained from measuring road profile by using 4 sensors of accelerometer placed on each car wheel. The measuring data is converted to be vertical displacement data by using a "double integrator", however, it is not easy to get accurate results since the signal obtained carries a lot of noise and it is necessary to design the right filter reduce the noise. In this study, the signal filtering methods reducing the noise were used Fast Fourier Transform (FFT) and Kalman Filter (KF) combination. Experiments were carried out by combining Fast Fourier Transform and Kalman Filters using an input signal with unit (volt) in the time domain. In addition, this research focused on preparing the survey data that has been obtained by eliminating the noise to convert becoming the displacement input data for providing the loads of automotive simulation testing.

Keywords: Road profiles; Acceleration data; Fast fourier transform; Kalman filter

1. Introduction

Vehicle mobility is without doubt a key element of the transportation system. High vehicle mobility must be supported by good road infrastructure, because this affects travel time and one of the road infrastructures that often suffers damage is the road profile [1]–[3]. The roughness of the road profile causes a number of problems for road users such as unsafe conditions for drivers, resulting in deteriorating dynamic conditions for large vehicles such as trucks or other heavy vehicles, and can damage the vehicles and goods being transported. One possibility that causes the road to experience high levels of roughness is segregation which affects pavement performance [4], [5]. A good road surface can provide safety and comfort for road users. It also reduces the number of car accidents and improves transportation safety. The quality of the road has become an important concern, in which, among various indicators of road quality, the road roughness is one of the most important road parameter [6]–[8]. While road surveys are necessary to obtain road data and maintain road quality, there are several different methods and tools for evaluating and characterizing road profiles. Accelerometers are one of the important devices for assessing the types of vibration modes including forced reaction systems [9], [10]. The surface road measurement includes determining the designated operational road of the vehicle, collecting the surface road data, and processing or preparing the data to be converted into the loading program for shaker test (**Figure 1**). The

sample load profile representing the displacement of four vehicle wheels given during the simulation test can be seen in **Figure 2**.

To measure the dynamic effect of the road on the car (i.e.: suspension – axle – unsprung mass and/or car body springs) can be carried out by using different measuring devices such as accelerometers, speed or displacement measuring devices or height laser/infrared/ ultrasonic speed sensing devices. These measuring equipment are applied to compile the vertical irregularity data of the road surfaces or the geometric parameters of the pavement by using a high-precision measuring and surveying system [11]–[13]. The analysis method in carrying out a combination of filter to filter of the input signal with unit value of volts from experimental road profile data should be converted into the displacements. Analysis of the signal and its associated frequency is the most important step to identify the nature of the signal. Signals are generally consisted of four types, namely linear signals, non-linear signals, stationary signals, and non-stationary signals [14]. Many related studies have been carried out to

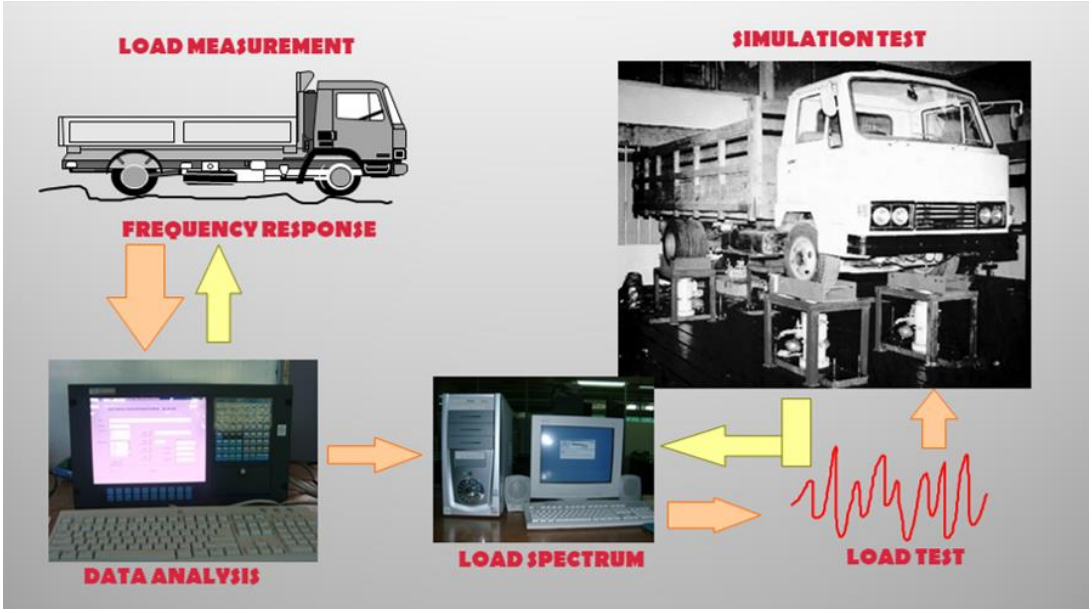

Figure 1. Simulation road test

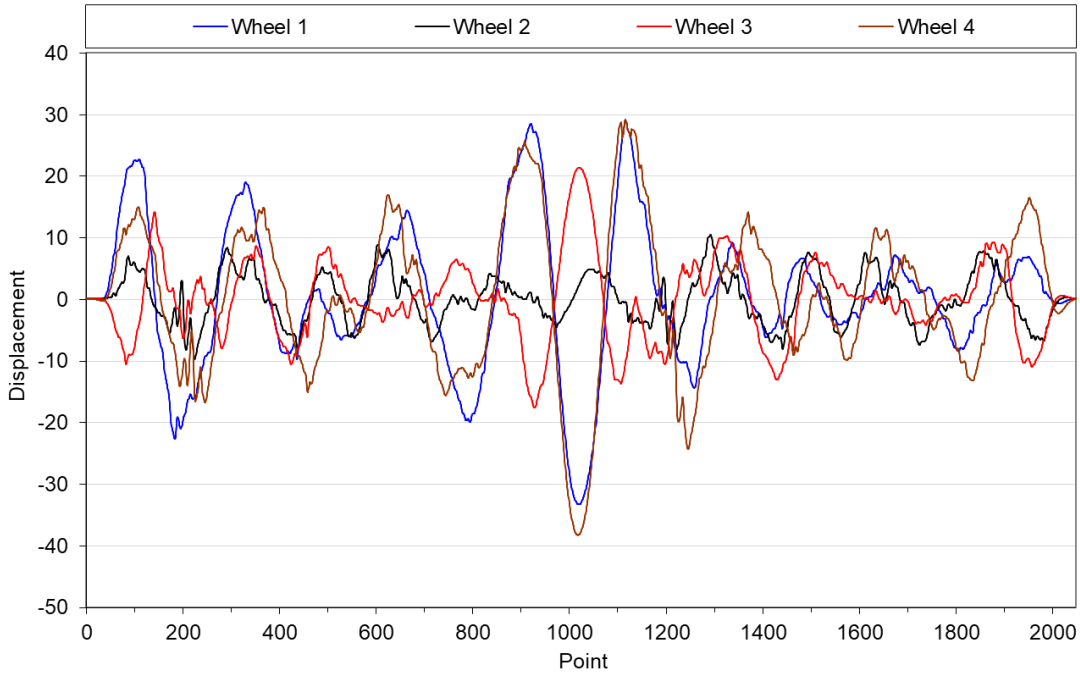

Figure 2. Sample load file (displacement vs point, DFHST4)

obtain the displacements using a Finite Impulse Response (FIR) filter to correct numerical integration and an Infinite Impulse Response (IIR) to process the frequency domain [15], [16]. In general, FIR and IIR can pass certain frequencies and noise clearly. In fact, it is very difficult to determine the perfect filter, therefore in this study trials were carried out with a combination of Fast Fourier Transform and Kalman Filters to perform noise separation and correct the velocity and displacement results [17]–[19].

Fast Fourier Transform (FFT) and Kalman Filter (KF) cannot filter to separate such filters as low, high, and band pass filters, however, FFT and KF have the ability to do filtering. The combined process of FFT and KF will be tested in this study to find out the results of road profile data analysis. The study goal is to analyze surface roughness road profile data using filter combinations determining the ability to solve the conversion problem from the measurement data becoming the displacements. The research focuses on the data from the road surface roughness measurements and the process for analyzing data using a combination of filters.

2. Related Works

Research related to simulate randomized longitudinal road profiles is widely used for various vibration analyzes of mechanical and civil structures. Common examples of the use of such simulations to evaluate vehicle vibration responses include optimizing vehicle or seat suspension, estimating energy harvesting and regeneration in vehicle suspension, to evaluate dynamic loads. sidewalks or vehicles [20]. Many research papers have investigated how classifying the road profiles accurately based on the classification through the number of axles and vehicle body. The acceleration data from various simulated dynamic vehicle-road scenarios by using accelerometers is a result data from measuring the vehicle's response to the road surface which is to be collected and stored as the acceleration measurement data for estimating average road profile conditions [21]–[23]. Information raw data is used to generate road surface classification by using two approaches, namely active and passive sensing. Active sensing sensors interact with the environment to generate data by using ultrasonic sensors, laser scanning, sonar and radar. The passive sensing has no active interaction with the environment and the data obtained by physical or visual are passive samples using camera and inertial sensors [24]–[26]. There are various methods and tools for measuring road surface characteristics which can be divided into three categories: system response base estimation, direct measurement, and non-contact measurement [27].

Some studies to measure the dynamic response of automotive structures employed accelerometers. This acceleration data is most often used to estimate speed and displacement. Velocity is an integral of acceleration, while displacement is an integral of velocity. Numerical methods allow obtaining results as discrete functions by integration. Direct integration of acceleration often results in unrealistic deviations in velocity and displacement, however, it is undoubtedly the most appropriate and most cost-effective way to get a converted data [28]–[30]. In this study, measuring dynamic automotive on road profile was used the accelerometers located on each wheel, and the collected measurement data was created at the survey location between Ciawi - Cisarua Puncak (10 km), Indonesia, as shown in **Figure 3**. Sample raw data of measurement is shown in **Figure 4**.

Various methods have been carried out to determine road roughness, such as the concept of an algebraic estimator to reconstruct a road profile with a minimum number of sensors, in which the algorithm only requires sprung and unsprung mass acceleration data. In addition to identify road profiles can be done by characterizing road excitation using independent component analysis (ICA). The method can reconstruct the original excitation source using physically measured signals from the system under this study. Therefore, the estimated road disturbance is considered as an output source and is identified from the dynamic response of the vehicle. These responses could include simple filters of a moving average or complicated mathematical transformations such as various Fourier and Wavelet transforms and simulated numerically using the Newmark method [31], [32]. The method for separating noise is done by using a modified discrete Fourier transform to filter noise and makes reductions on the data while keeping the trend of the global movement of the time series

Figure 3. Survey location between Ciawi - Cisarua Puncak (10 km) in West Java, Indonesia

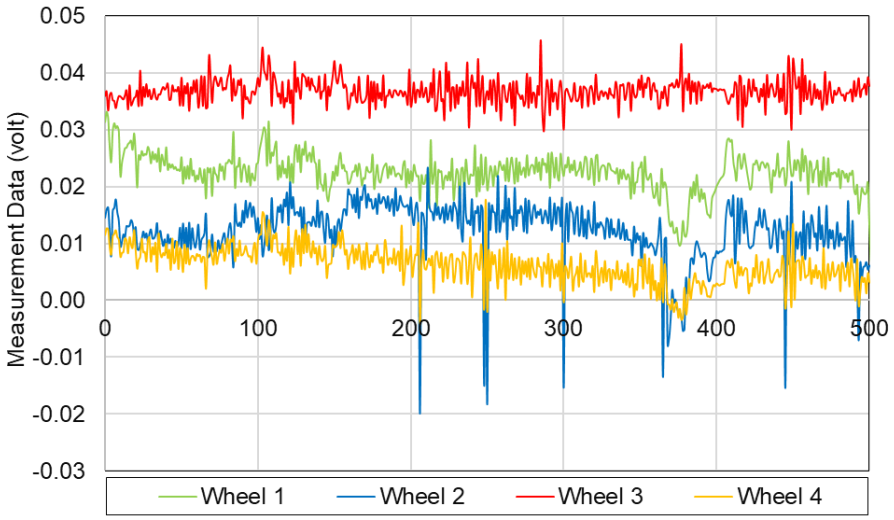

Figure 4. Sample raw measurement data

A promising method is a technique that performs data reduction, and then uses a spatial access method to index the data in the transformation space. The technique included the discrete Fourier transform (DFT) which was introduced in the study [33].

3. Methodology

The methodology for analyzing road profile data with a combination of filters was started by analyzing raw data obtained from the results of road profile survey by using 4 accelerometer sensors mounted on all four vehicle wheels. Data captured by the accelerometer sensor in volts was then converted into m/s² with equivalent conversion (1G = 0.002 Volts). The resampling of raw data was done to simplify data processing. In this study, down sampling was carried out, from one million rows by using the aggregate average in each 2000 row of data to 512 row data. The resampling data is shown in **Figure 5**, in which the vertical axis is acceleration in m/s² and the horizontal axis is data numbers.

Fast Fourier Transform (FFT) is a method to speed up calculation time. This is compared by using the Discrete Fourier Transform, where datasets in the time domain are converted into the frequency domain. In this study, the use of FFT aims to reduce noise that occurs when measurements are taken, and the choice of this method is due to its ease of use and accurate results. By using the FFT method, the calculation process is begun with converting 512 data values in units of volts into m/s², where 1G = 0.002 volts.

The next stage is to process filtering accelerometer data by FFT, then to integrate the accelerations to get speed results [34]–[37]. To give confidence in the accuracy of the speed values, the results data is treated by using the Kalman Filter to get an estimation of the speed values approaching the actual values. Then, the output of Kalman Filter is integrated to become the displacement data values. The process transforming raw acceleration measuring data converted to be the displacement road profile simulation data by using FFT dan Kalman Filter is shown in flowchart diagram **Figure 6**.

As an illustration of the FTT process in **Figure 6**, the acceleration data should be examined into two, namely even data and odd data, and formulated as Eq (1) [34]. Calculations were made on 512 data using FFT through the W matrix (256 x 256) for odd and even parts. The calculation results of FFT are complex numbers, and as an illustrative example from **Figure 5** wheel 1, for k = 1 by resampling the initial data 162.888, the calculation result is a complex number of -218,907 - j1599,802. While the magnitude of the complex number is 1614.71. Calculations are continued for all data (i.e., 512 data).

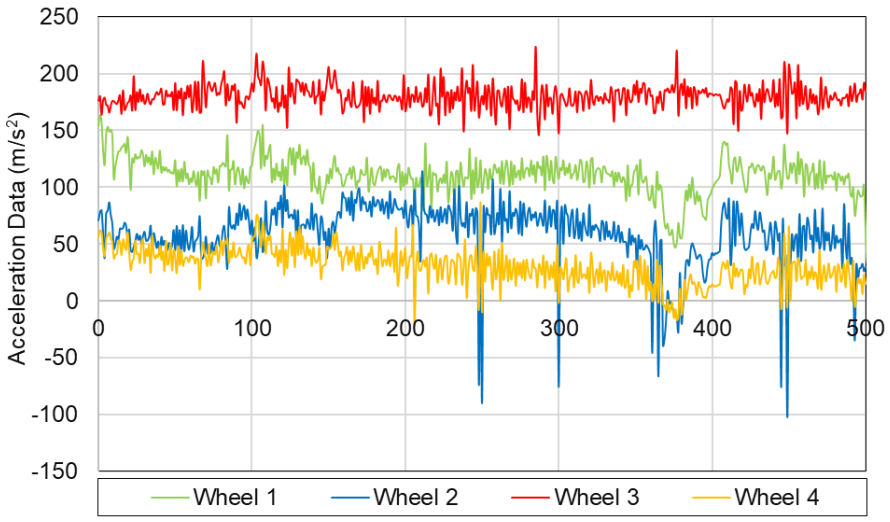

Figure 5. Resampling acceleration data

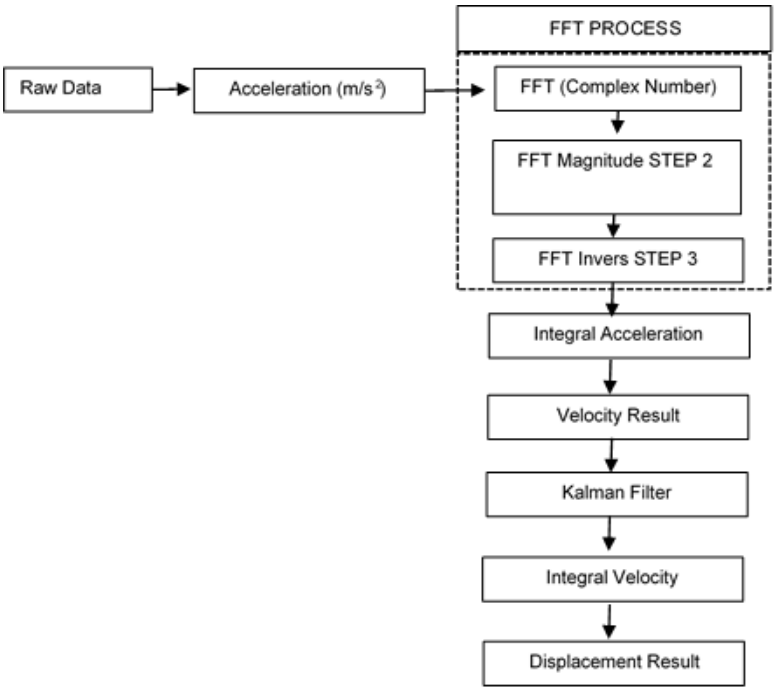

Figure 6. Processing Transformation Flowchart from row acceleration data to displacement data

$$X_k = \frac{1}{N}\left(\sum_{n=0}^{\frac{N}{2}-1} x(2n) \times W_{\frac{N}{2}}^{nk} + W_N^k \sum_{n=0}^{\frac{N}{2}-1} x(2n+1) \times W_{\frac{N}{2}}^{nk}\right) \quad (1)$$

where:

$W = e^{-i\frac{2\pi}{N}}$; first component or $\sum_{n=0}^{\frac{N}{2}-1} x(2n) \times W_{\frac{N}{2}}^{nk}$ is even part; and $\sum_{n=0}^{\frac{N}{2}-1} x(2n+1) \times W_{\frac{N}{2}}^{nk}$ is odd part.

In the FFT process **Figure 6**, the frequency domain of the output of FFT process is the complex number value$(a + j\,b)$, namely step 1. Then, step 2 the format complex number is modified to be magnitude and phase form, i.e., magnitude $A = \sqrt{(a^2 + b^2)}$ and phase angle $\theta = \tan^{-1}(a/b)$. And step 3 the process continues to inverse FFT calculation, so that the result value is returned to the time domain as the same format of initial data.

The acceleration data (a) can be converted to the velocity data (v) by using the following integral Eq (2):

$$v = \int_1^t a\, dt \quad (2)$$

Second filter to remove the noise of velocity data is done by using Kalman Filter [38]–[40]. The data processed in the Kalman Filter is the velocity data as the integration result of acceleration data. In contrast to the FFT, the Kalman Filter is applied to eliminate the noise and improve the velocity result data approaching the actual values. To implement the Kalman Filter, it is initiated by defining data variables such as the velocity data. The variable state transition model is assumed that the relative velocities in between constant measurements are developed from time to time. The velocity can be expressed as $v(k) = v(k-1)$, where $v(k)$ is velocity at time k and $v(k-1)$ is velocity at the previous time. The measurement model related to velocity variable is $z(k) = v(k)$, where $z(k)$ represents the measured velocity at time k. The initial values are assumed $x(0) = 4.0$, error covariance matrix $P(0)$ and noise covariance R.

For each measurement data at time k, the steps taken should be distinguished as following state parameters:

a. State prediction:

$$x(k|k-1) = x(k-1) \quad (3)$$

b. State prediction:

$$P(k|k-1) = P(k-1) \quad (4)$$

c. State update Kalman Filter Gain:

$$K(k) = P(k|k-1) \,/\, (P(k|k-1) + R) \quad (5)$$

where R is measurement noise covariance

d. State update Estimation:

$$x(k|k) = x(k|k-1) + K(k) * (z(k) - x(k|k-1)) \quad (6)$$

e. State update covariance:

$$P(k|k) = (1 - K(k)) * P(k|k-1) \quad (7)$$

These steps have to be repeated for each measurement. The magnitude of the filtered values is given by $x(k|k)$ at any time k, where these values are values obtained based on the estimated speed at time k.

The final step is to convert the velocity data (v) to displacement data (x) in the time domain (t) by using the following Eq (8).

$$x = \int_1^t v\, dt \quad (8)$$

The integral results of the velocity data can be applied as the input displacement data for the loading program of simulation road profile automotive testing. The input loading is given to each actuator supporting each vehicle wheel as shown in **Figure 1** and **Figure 2**.

4. Analysis and Discussion

The number of data row from the field survey is 1 million rows as the results of measurements using an accelerometer mounted on each wheel of four wheels vehicle. Data resampling is part of the data processing of 1 million data in units of volt, which is then converted to m/s^2 with an equivalence value (1G = 0.002 Volts). Down sampling was carried out, from one million rows

by using the aggregate average in each 2000 rows of data to 512 rows data (Figure 4 and Figure 5).

To detect the noise or inconsistency of raw data, it can be done through the histogram as shown in Figure 7 and Figure 8 the histograms of measurement data and displacement data, consecutively, so that the number of extreme values indicates the noise.

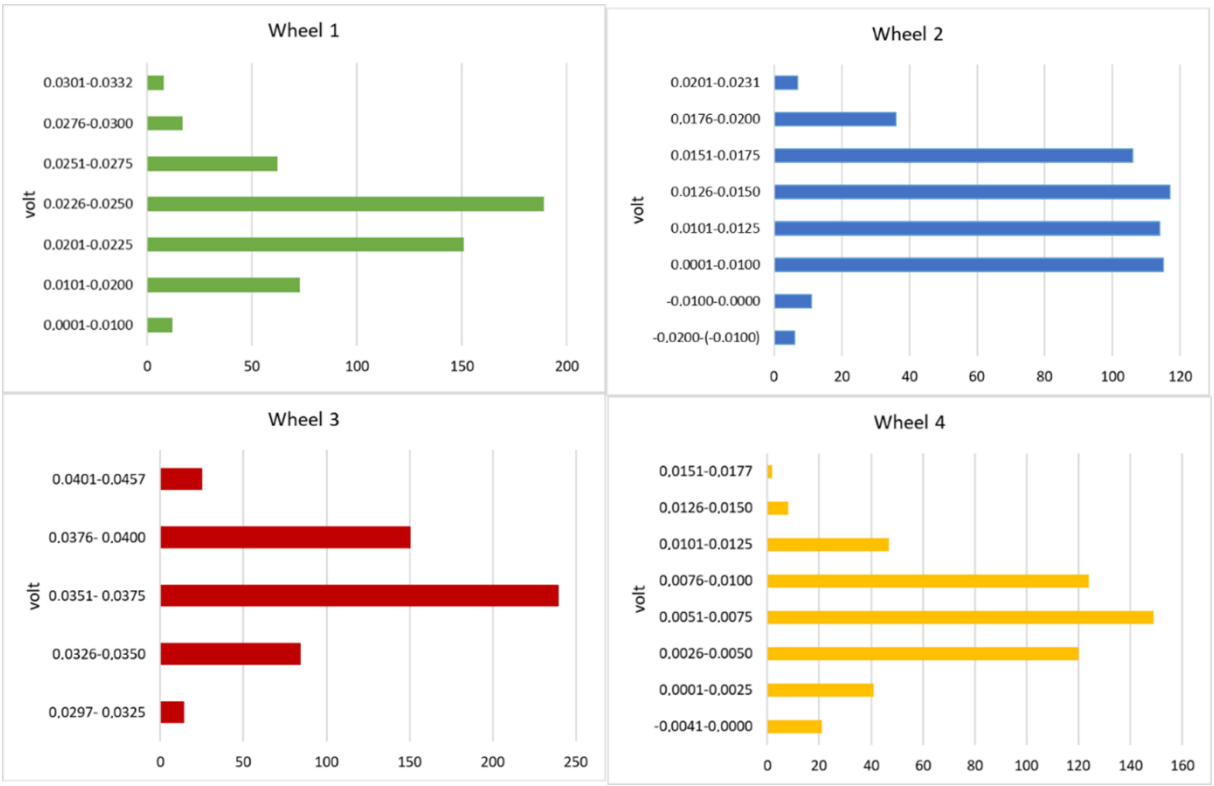

Figure 7. Histogram of measurement data

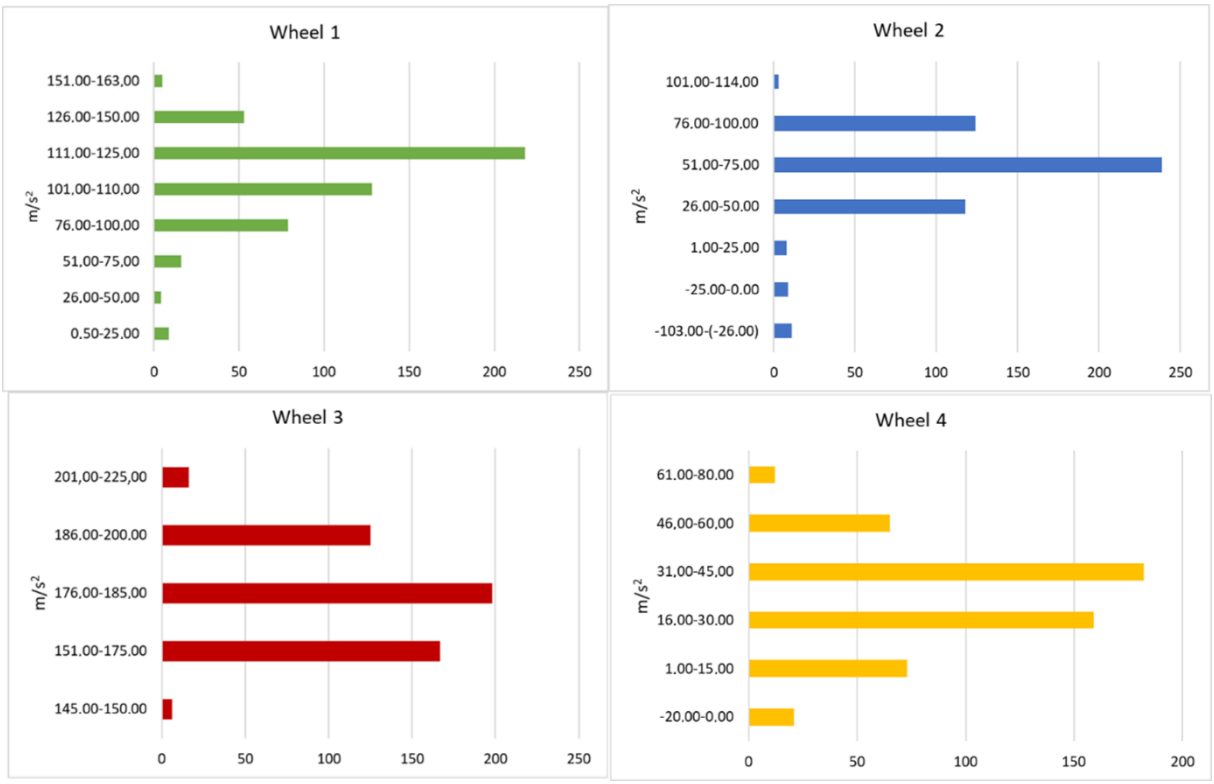

Figure 8. Histogram of acceleration data

The numbers of extreme values in the measurement data and acceleration conversion are shown at the maximum and minimum value intervals in **Figure 7** and **Figure 8**, while the position of the noise or extreme values can be seen in **Figure 4** for the measurement data and **Figure 5** for the acceleration conversion. The extreme values of the measurements (**Figure 7**) have negative values with intervals of -0.0199 volts to 0 volts recorded on wheels 2 and 4, where on wheel 2 there are 6 peak values between -0.0199 volts to -0.0135 volts. Meanwhile, negative values in acceleration data are similar to measurement data, where negative values occur in wheels 2 and 4 with intervals of -103 m/s^2 – 0 m/s^2 (**Figure 8**). Meanwhile, positive extreme values occur in data wheel 3 with intervals from 0.0401 to 0.0457 volts from measurement data and 201 to 225 m/s^2 in wheel 3 of acceleration data.

The extreme values or noise can be reduced by computing as follows on the FFT method to become new acceleration data (**Figure 9** and **Figure 10**). The noise number has decreased significantly, in which there is no negative value and the only first data value of each wheel has the extreme value, i.e. > 200 m/s^2 . The distribution of acceleration data values is more even and concentrated in the interval of the median value of each wheel. Data values of wheel 1, 2, 3, and 4 are concentrated at intervals of 88 to 120 m/s^2, 30 to 80 m/s^2, 170 to 190 m/s^2, and 10 to 50 m/s^2, consecutively. With a more even distribution values, the noise is reduced and the integration process can be carried out to estimate the velocity data values.

The output data in **Figure 9**, based on the movement of the test vehicle, describes that the sensor positions of wheels 1 and 3 at the front and rear wheels respectively, but the axles are different. These are similarly with wheels 2 and 4. From point of viewed general road surface, the same surface is traversed by wheels 1 and 3, and also the other side road surface is traversed by wheels 2 and 4. The accelerometer mounted on each wheel captures signals from the movement of the wheels and these signals are converted in units of volts. The results of filtering using the FFT indicate that there is a fairly large spike of each measured wheel data at the time of initial moving vehicle. Each wheels give a signal to each accelerometer in the form of voltage (volts) and the initial movement of the vehicle gives a shock signal to the accelerometer so that the output voltage has quite large value. After a normally running vehicle (about 10 seconds), the accelerometer has been able to adapt road signals. The results of noise separation using the FFT show that the acceleration data within a time span of 512 seconds is closed to the real conditions. Overall, the acceleration trend of the 4 wheels, especially wheels 1 and 3, as well as wheels 2 and 4, are almost the same.

Figure 10 shows the histogram of the FFT output of all 512 acceleration data values in which the condition of the road surface traversed by the 4 wheels of the test vehicle has different total frequent acceleration values. Differences in acceleration values occur between wheels 1 and 3 as well as wheels 2 and 4 even though they generally cross on the same road surface. The

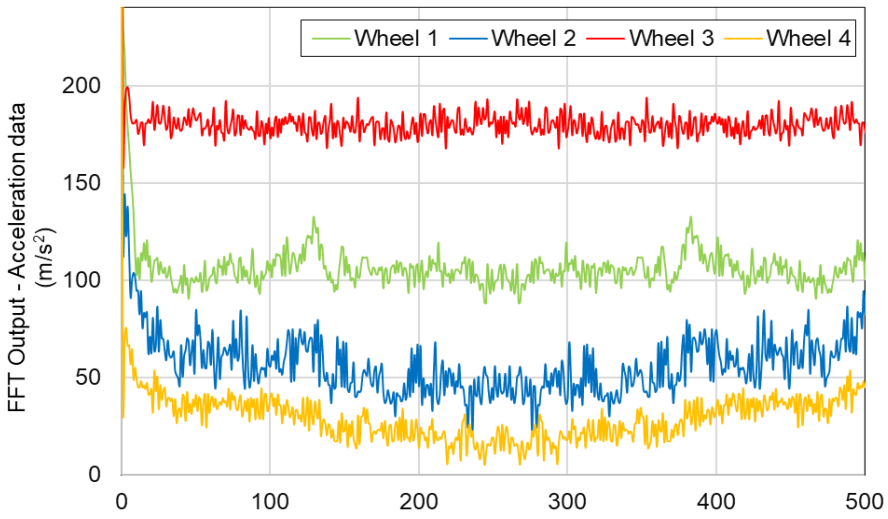

Figure 9. Acceleration data as output of FFT process

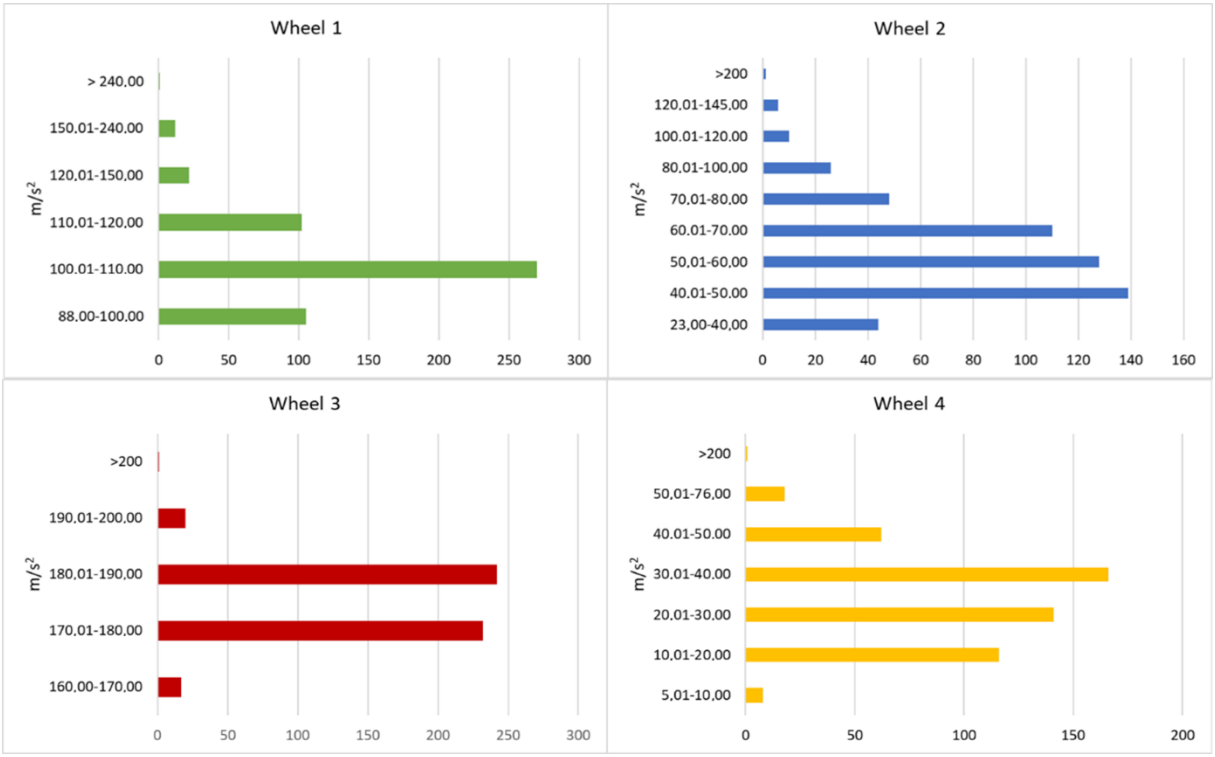

Figure 10. Histogram of FFT output

potential different values can be caused by differences in the trajectories traversed by wheels 1 and 3 as well as wheels 2 and 4, environmental influences such as dust, dirt around the installed accelerometer, and the accelerometer equipment used has a different level of precision and sensitivity due to installation. These can be seen that wheels 1 and 3 have different acceleration values where the acceleration value of wheel 3 is higher than wheel 1, and so does with wheels 2 and wheel 4 where the acceleration of wheel 2 is higher than that of wheel 4, but the acceleration trend of wheel 1 and 3 as well as wheel 2 and 4 have almost the same trend.

This data is integrated by using Eq (2) to transform becoming the velocity data as shown in **Figure 11** and **Figure 12**. **Figure 11** shows velocity graphs, where the input data of filtering acceleration values using FFT has been processed, and the results are approaching to real mode and values of acceleration data. Then, the next process is a mathematical process where the acceleration values are integrated to produce velocity signals, in which there are graphically no significant changes. The wheels 1 and 3 as well as wheels 2 and 4 only experience change in the magnitude of the velocity values and their units while the velocity trend graphs remain the same.

Figure 12 shows the velocity histogram, where the peak velocity values that most often appear in the time span of 512 velocity values can be describe as the velocity frequent values between 3.21 - 3.4 m/s of wheel 1, 1.51 - 2 .00 m/s of wheel 2, 5.61 - 5.80 m/s of wheel 3, and 0.81 - 1.20 m/s of wheel 4 are 186, 194, 214, and 205 times, consecutively. The velocity values and frequent number are obtained as the result of a mathematical process due to integral acceleration data. The mathematical processes that occur between wheels 1 and 3 as well as wheels 2 and 4 cause differences in the magnitudes of velocity. These occur following changes in the input acceleration data, while the velocity modes have the same trend of the acceleration graphs.

The results of filtered velocity by using the Kalman Filter are shown in **Figure 13** and **Figure 14**. This second filter is used to reduce the remaining noise. In general, applying the Kalman filter method, the estimated velocity values are almost the same to the velocity values as the integration results of acceleration data indicating that the input velocity values have insignificant noise. The results of filtering on wheels 1 and 3 do not experience large changes in their velocity values as well as those of wheels 2 and 4. The velocity graphs, before and after processed through

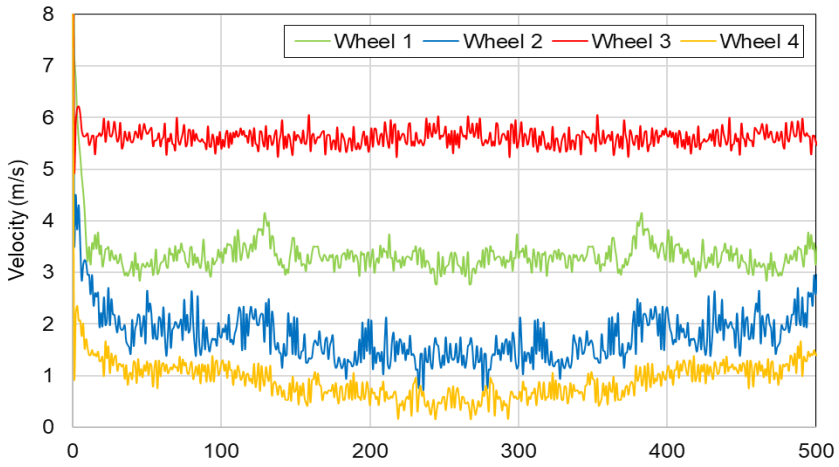

Figure 11. Velocity as integral output of accelerometer data

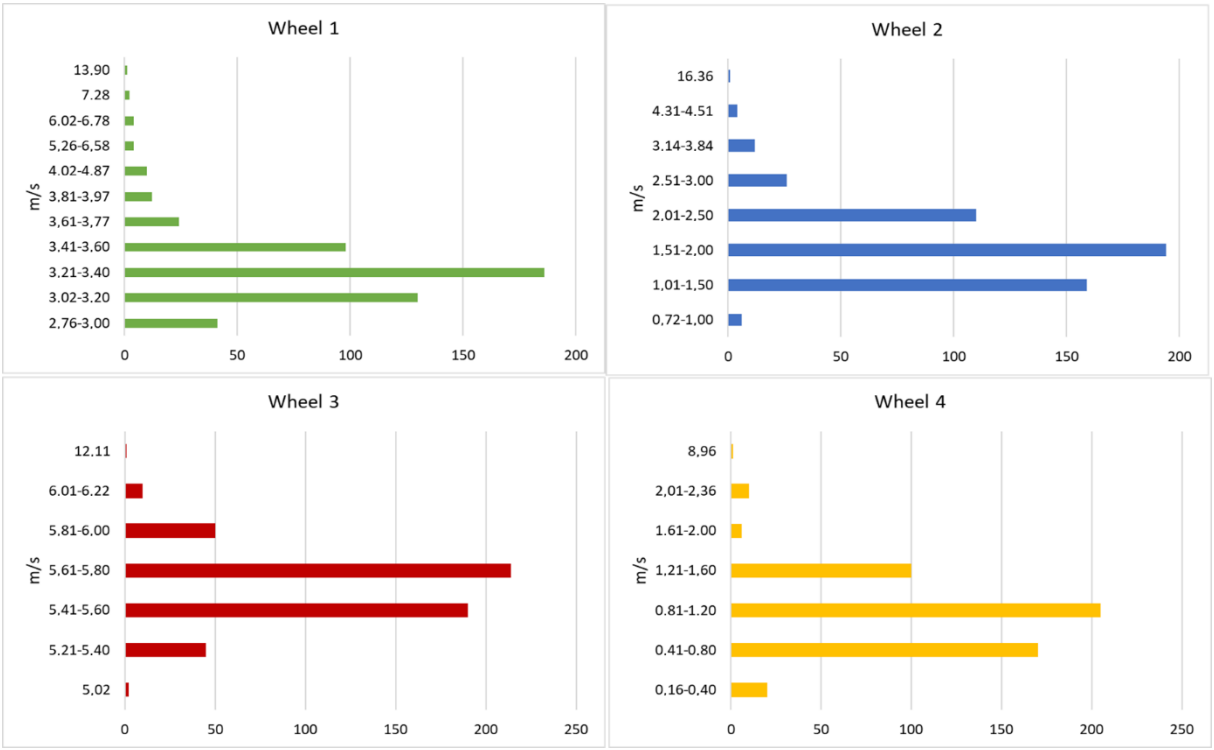

Figure 12. Velocity histogram as integral output

Kalman Filter on wheels 1 and 3 as well as wheels 2 and 4 are almost the same modes and magnitudes (**Figure 13**).

Figure 14 shows the speed histogram of the Kalman filter results, where the happen frequent velocity values of each wheel among 512 peak velocity values are the velocities of wheel 1 between 2.41 - 2.80 m/s, wheel 2 in between 0.01 - 0.50 m/s, wheel 3 in between 6.01 - 6.25 m/s, wheel 4 in between -1.50 – (-1.01) m/s have the peak number of 242, 178, 161, 198 times, successively. The results of Kalman Filter Process show that wheels 1 and 3 as well as wheels 2 and 4 have only small differences in the magnitudes of velocity value, while the graphical velocity trends are similar between wheels 1 and 3 as well as wheels 2 and 4.

The displacement values as a result of the velocity integral are shown in **Figure 15** and **Figure 16**. The two-time filtering processes using the FFT and Kalman Filter have been done to reduce the noise for obtaining the velocity values. The displacement graphics of wheels 1 and 3 as well as wheels 2 and 4 are similar the velocity graphs but different on unit system, due to the mathematical process of integration method.

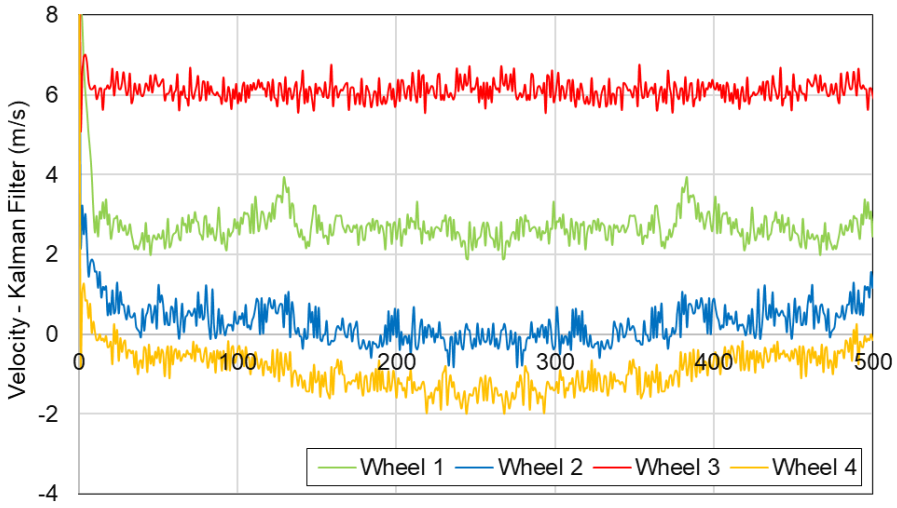

Figure 13. Velocity as output of Kalman Filter

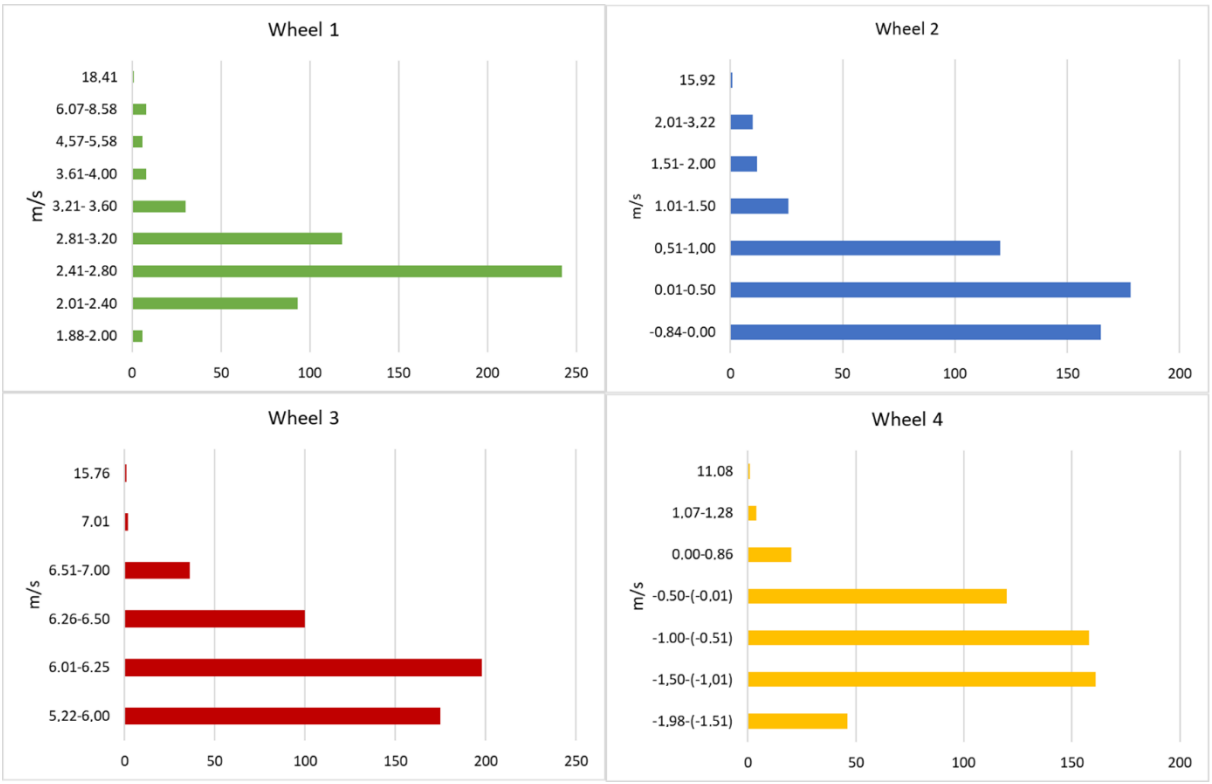

Figure 14. Velocity histogram Kalman Filter

The initial displacement values in **Figure 15** have quite high magnitudes since these values follow the accelerometer output data. The raw data as the first input of subsequent processes reducing the noise is carried out only up to a certain limit where the potential for lost real data can be reduced, and at the end of the process, the displacement data has fairly high values. This result is indicated due to the influence of the accuracy and sensitivity of the accelerometer when the measurement starts and stops suddenly.

The displacement values on wheels 1 and 3 as well as wheels 2 and 4 do not affect the trend of the displacement graph (**Figure 15**), in which the only changes are in the magnitude values and unit length (m) (**Figure 16**). The most frequent peak values of wheel 1, 2, 3 and 4 are 0.08 m for 194 times, 0 m for 134 times, 0.19 m for 248 times, and -0.03 m (-0.02 m) for 113 times (112 times), consecutively. In general, the difference peak value of wheels 1 and 3 is 0.11 m, while wheels 2 and 4 is 0.03 m. The potential sources for these

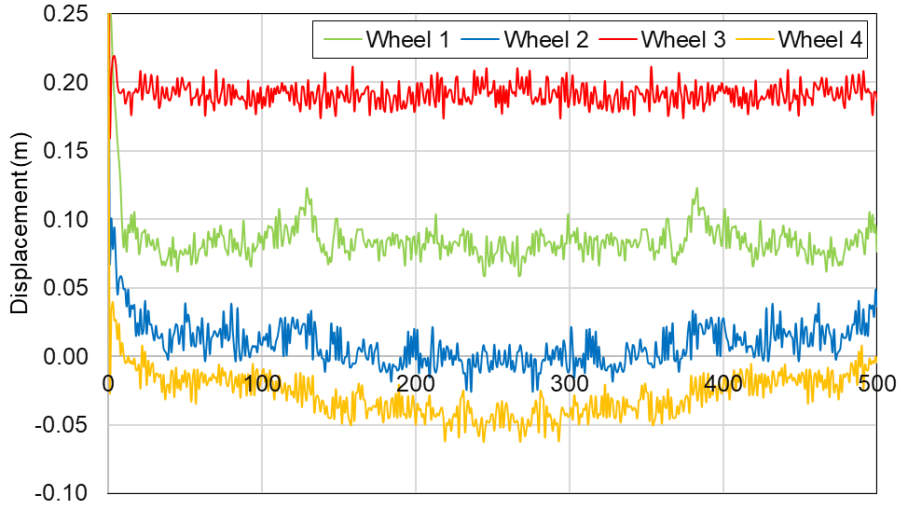

Figure 15. Displacement as integral output of velocity

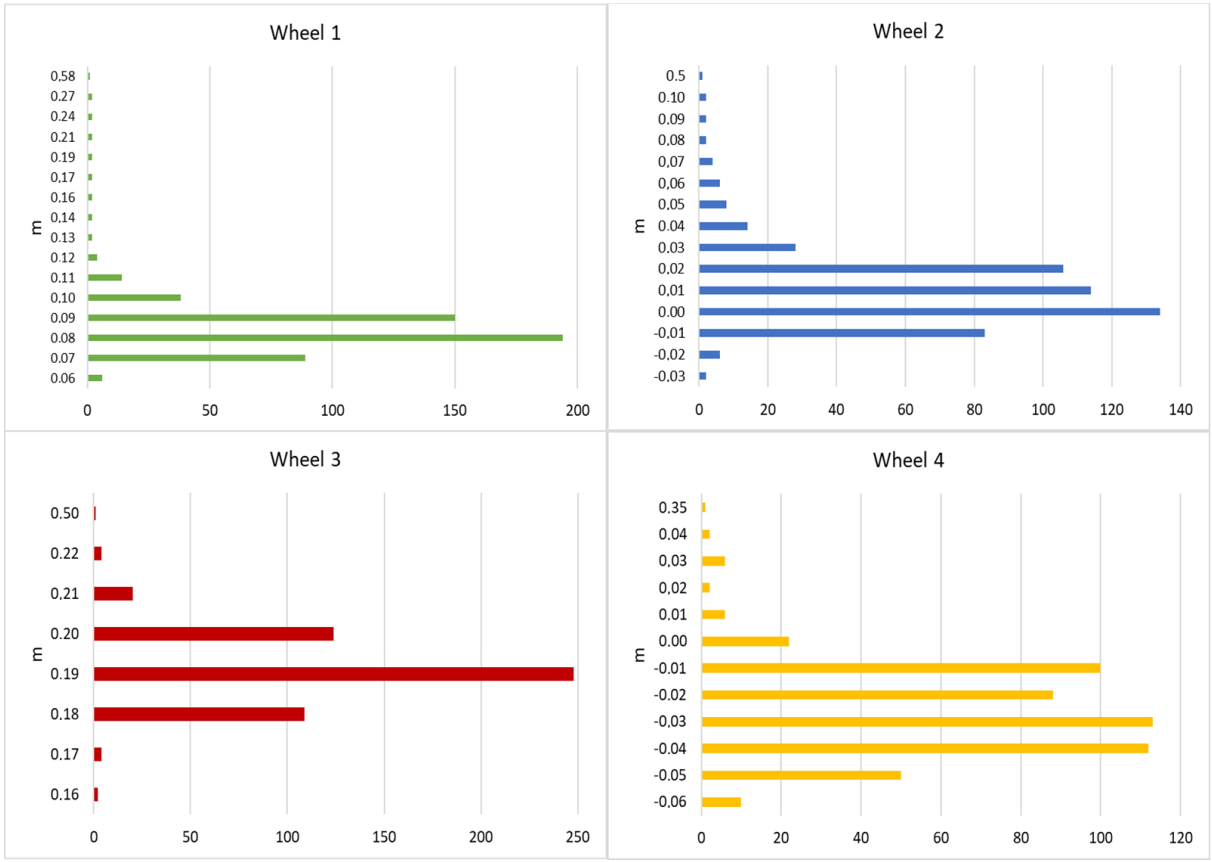

Figure 16. Displacement histogram

differences are affected such as the road paths traversed by wheels 1 and 3 (left-front and rear) and wheels 2 and 4 (right-front and rear) not necessarily the same location, and environmental influences such as dust, dirt, watery roads, and also the conditions of each accelerometer with different levels of accuracy and sensitivity considering the different locations where they are installed.

5. Conclusion

a. The combined processes of FFT and KF are tested in this study to find out the results of road profile data analysis and the study goal is to solve the conversion problem from the measurement data becoming the displacements.

b. In the filter design for converting acceleration into displacement, it shows that the FFT filter

plays a more significant role in filtering, so the filter reduces the noise of displacement data significantly.

c. In this experiment, the Kalman filter was not modified the velocity data significantly, so it seemed that the filter makes a small contribution to reduce the noise and distortion that occurred.

d. The input acceleration data values wheel 1, 2, 3, and 4 are concentrated at intervals of 88 to 120 m/s^2, 30 to 80 m/s^2, 170 to 190 m/s^2, and 10 to 50 m/s^2, consecutively. And the most frequent filtered displacement peak values of wheel 1, 2, 3 and 4 are 0.08 m for 194 times, 0 m for 134 times, 0.19 m for 248 times, and -0.03 m (-0.02 m) for 113 times (112 times), successively.

Acknowledgement

We acknowledge National Research and Innovation Agency for supporting this research.

Author's Declaration

Authors' contributions and responsibilities

Djoko W. Karmiadji: Concept, Methodology, Numerical Analysis and Conclusion; Tri Widodo: Fast Fourier Transform (FFT) Data Analysis and FFT Theory; Rosyidi: Kalman Filter Analysis and Kalman Filter Theory; Harris Zenal: Hardware Accelerometer specialist for survey needs; Nofriyadi Nurdam: Compile a Flow Chart for coding Kalman Filter and Kalman Filter Theory; Sahid Bismantoko: Compile a Flow Chart for FFT coding and FFT Theory; Andi M. Kadir: Displacement Mechanical Theory in implementing Accelerometer utilization; Sofwan Hidayat: Analysis and compilation of data from field survey results; Nurhadi Pramana: Theory and References related to the use of the Accelerometer for Road Profile survey needs; Winarno: Theory and related references remove noise from field survey data.

Funding

No funding provides for this article from the institution or agency.

Availability of data and materials

All data are available from the authors.

Competing interests

The authors declare no competing interest.

Additional information

No additional information from the authors.

References

[1] E. Šabanovič, V. Žuraulis, O. Prentkovskis, and Viktor Skrickij, "Identification of Road-Surface Type Using Deep Neural Networks for Friction Coefficient Estimation." Sensors 2020, doi: ; doi:10.3390/s20030612.

[2] P. Johannesson, K. Podgórski, and I. Rychlik, "Modelling roughness of road profiles on parallel tracks using roughness indicators," *International Journal of Vehicle Design*, vol. 70, no. 2, pp. 183–210, 2016, doi: 10.1504/IJVD.2016.074421.

[3] T. Rateke and A. von Wangenheim, "Road surface detection and differentiation considering surface damages," *Autonomous Robots*, vol. 45, no. 2, pp. 299–312, 2021, doi: 10.1007/s10514-020-09964-3.

[4] A. Arunika, J. F. Fatriansyah, and V. A. Ramadheena, "Detection of Asphalt Pavement Segregation Using Machine Learning Linear and Quadratic Discriminant Analyses," *Evergreen*, vol. 9, no. 1, pp. 213–218, 2022, doi: 10.5109/4774236.

[5] P. Marcelino, M. de Lurdes Antunes, E. Fortunato, and M. C. Gomes, "Machine learning approach for pavement performance prediction," *International Journal of Pavement Engineering*, vol. 22, no. 3, pp. 341–354, 2021, doi: 10.1080/10298436.2019.1609673.

[6] K. Zang, J. Shen, H. Huang, M. Wan, and J. Shi, "Assessing and mapping of road surface roughness based on GPS and accelerometer sensors on bicycle-mounted smartphones," *Sensors (Switzerland)*, vol. 18, no. 3, 2018, doi: 10.3390/s18030914.

[7] P. Múčka, "Vibration Dose Value in Passenger Car and Road Roughness," *Journal of Transportation Engineering, Part B: Pavements*, vol. 146, no. 4, 2020, doi: 10.1061/jpeodx.0000200.

[8] E. Kurakina, S. Evtiukov, and J. Rajczyk, "Forecasting of road accident in the DVRE system," *Transportation Research Procedia*, vol. 36, no. SPbOTSIC, pp. 380–385, 2018, doi: 10.1016/j.trpro.2018.12.111.

[9] O. G. Dela Cruz, C. A. Mendoza, and K. D. Lopez, "International Roughness Index as Road Performance Indicator: A Literature Review," *IOP Conference Series: Earth and Environmental Science*, vol. 822, no. 1, 2021, doi: 10.1088/1755-1315/822/1/012016.

[10] E. Ranyal, A. Sadhu, and K. Jain, "Road Condition Monitoring Using Smart Sensing

and Artificial Intelligence: A Review," *Sensors*, vol. 22, 2022, doi: https://doi.org/10.3390/s22083044.

[11] S. Eshkabilov, "Measuring and Assessing Road Profile by Employing Accelerometers and IRI Assessment Tools," *American Journal of Traffic and Transportation Engineering*, vol. 3, no. 2, p. 24, 2018, doi: 10.11648/j.ajtte.20180302.12.

[12] F. Rezaei, "Laser Doppler vibrometer and accelerometer for vibrational analysis of the automotive components during Simulink simulation for validation," pp. 1–18.

[13] A. A. Youssef, N. Al-Subaie, N. El-Sheimy, and M. Elhabiby, "Accelerometer-based wheel odometer for kinematics determination," *Sensors (Switzerland)*, vol. 21, no. 4, pp. 1–32, 2021, doi: 10.3390/s21041327.

[14] P. Gupta, B. Singh, and Y. Shrivastava, "Robust Techniques for Signal Processing: A Comparative Study," *Evergreen*, vol. 9, no. 2, pp. 404–411, 2022, doi: 10.5109/4794165.

[15] S. M. S Rocha, J. S. Flávio Feiteira, P. S. N Mendes, U. P. B Da Silva, and R. F. Pereira, "Method to Measure Displacement and Velocityfrom Acceleration Signals," *Journal of Engineering Research and Application www.ijera.com*, vol. 6, no. 6, pp. 52–59, 2016.

[16] V. N. Stavrou, I. G. Tsoulos, and N. E. Mastorakis, "Transformations for fir and iir filters' design," *Symmetry*, vol. 13, no. 4, pp. 1–9, 2021, doi: 10.3390/sym13040533.

[17] F. Naseri, Z. Kazemi, E. Farjah, and T. Ghanbari, "Fast Detection and Compensation of Current Transformer Saturation Using Extended Kalman Filter," *IEEE Transactions on Power Delivery*, vol. 34, no. 3, pp. 1087–1097, 2019, doi: 10.1109/TPWRD.2019.2895802.

[18] A. K. Singh and B. C. Pal, "Rate of Change of Frequency Estimation for Power Systems Using Interpolated DFT and Kalman Filter," *IEEE Transactions on Power Systems*, vol. 34, no. 4, pp. 2509–2517, 2019, doi: 10.1109/TPWRS.2018.2881151.

[19] J. Zhang, Y. Liu, H. Liu, and J. Wang, "Learning local–global multiple correlation filters for robust visual tracking with kalman filter redetection," *Sensors (Switzerland)*, vol. 21, no. 4, pp. 1–20, 2021, doi: 10.3390/s21041129.

[20] P. Múčka, "Simulated road profiles according to ISO 8608 in vibration analysis," *Journal of Testing and Evaluation*, vol. 46, no. 1, pp. 405–418, 2018, doi: 10.1520/JTE20160265.

[21] M. Arbabpour Bidgoli, A. Golroo, H. Sheikhzadeh Nadjar, A. Ghelmani Rashidabad, and M. R. Ganji, "Road roughness measurement using a cost-effective sensor-based monitoring system," *Automation in Construction*, vol. 104, no. May 2018, pp. 140–152, 2019, doi: 10.1016/j.autcon.2019.04.007.

[22] M. M. Chaabane, D. Ben Hassen, M. S. Abbes, S. C. Baslamisli, F. Chaari, and M. Haddar, "Road profile identification using estimation techniques: Comparison between independent component analysis and Kalman filter," *Journal of Theoretical and Applied Mechanics (Poland)*, vol. 57, no. 2, pp. 397–409, 2019, doi: 10.15632/jtam-pl/104592.

[23] S. Sattar, S. Li, and M. Chapman, "Developing a near real-time road surface anomaly detection approach for road surface monitoring," *Measurement: Journal of the International Measurement Confederation*, vol. 185, no. August, p. 109990, 2021, doi: 10.1016/j.measurement.2021.109990.

[24] P. Behera, A. Siddique, T. S. Delwar, M. R. Biswal, Y. Choi, and J. Y. Ryu, "A Novel 65 nm Active-Inductor-Based VCO with Improved Q-Factor for 24 GHz Automotive Radar Applications," *Sensors*, vol. 22, no. 13, pp. 1–18, 2022, doi: 10.3390/s22134701.

[25] J. Keenahan, Y. Ren, and E. J. OBrien, "Determination of road profile using multiple passing vehicle measurements," *Structure and Infrastructure Engineering*, vol. 16, no. 9, pp. 1262–1275, 2020, doi: 10.1080/15732479.2019.1703757.

[26] B. Zhao, T. Nagayama, and K. Xue, "Road profile estimation, and its numerical and experimental validation, by smartphone measurement of the dynamic responses of an ordinary vehicle," *Journal of Sound and Vibration*, vol. 457, pp. 92–117, 2019, doi: 10.1016/j.jsv.2019.05.015.

[27] J. Menegazzo and A. Von Wangenheim, "Multi-Contextual and Multi-Aspect Analysis for Road Surface Type Classification through Inertial Sensors and Deep Learning," *Brazilian Symposium on*

Computing System Engineering, SBESC, vol. 2020-Novem, 2020, doi: 10.1109/SBESC51047.2020.9277846.

[28] X. Xiao, Z. Sun, and W. Shen, "A Kalman filter algorithm for identifying track irregularities of railway bridges using vehicle dynamic responses," *Mechanical Systems and Signal Processing*, vol. 138, p. 106582, 2020, doi: 10.1016/j.ymssp.2019.106582.

[29] F. Liu, S. Gao, and S. Chang, "Displacement estimation from measured acceleration for fixed offshore structures," *Applied Ocean Research*, vol. 113, no. January, p. 102741, 2021, doi: 10.1016/j.apor.2021.102741.

[30] Y. Yang, Y. Zhao, and D. Kang, "Integration on acceleration signals by adjusting with envelopes," *Journal of Measurements in Engineering*, vol. 4, no. 2, pp. 117–121, 2016.

[31] G. Guo, H. Wang, and D. Bell, "Data reduction and noise filtering for predicting times series," *Lecture Notes in Computer Science (including subseries Lecture Notes in Artificial Intelligence and Lecture Notes in Bioinformatics)*, vol. 2419, no. June 2014, pp. 421–429, 2002, doi: 10.1007/3-540-45703-8_39.

[32] S. Pourzeynali, X. Zhu, A. G. Zadeh, M. Rashidi, and B. Samali, "Comprehensive study of moving load identification on bridge structures using the explicit form of newmark-β method: Numerical and experimental studies," *Remote Sensing*, vol. 13, no. 12. 2021, doi: 10.3390/rs13122291.

[33] M. Mastriani, "Quantum-Classical Algorithm for an Instantaneous Spectral Analysis of Signals: A Complement to Fourier Theory," *Journal of Quantum Information Science*, vol. 08, no. 02, pp. 52–77, 2018, doi: 10.4236/jqis.2018.82005.

[34] M. T. Heideman, D. H. Johnson, and C. S. Burrus, "Gauss and the History of the Fast Fourier Transform," *IEEE ASSP Magazine*, vol. 1, no. 4, pp. 14–21, 1984, doi: 10.1109/MASSP.1984.1162257.

[35] J. W. Cooley, P. A. W. Lewis, and P. D. Welch, *The Fast Fourier Transform and its Applications*, vol. 12, no. 1. 1969.

[36] A. González, E. J. O'Brien, Y. Y. Li, and K. Cashell, "The use of vehicle acceleration measurements to estimate road roughness," *Vehicle System Dynamics*, vol. 46, no. 6, pp. 483–499, 2008, doi: 10.1080/00423110701485050.

[37] M. Haddar, S. C. Baslamisli, R. Chaari, F. Chaari, and M. Haddar, "Road profile identification with an algebraic estimator," *Proceedings of the Institution of Mechanical Engineers, Part C: Journal of Mechanical Engineering Science*, vol. 233, no. 4, pp. 1139–1155, 2019, doi: 10.1177/0954406218767470.

[38] F. Tusell, "Kalman Filtering in R," *Journal of Statistical Software*, vol. 1, no. 1, pp. 128–129, 2009, doi: 10.1002/wics.10.

[39] Q. Li, R. Li, K. Ji, and W. Dai, "Kalman filter and its application," *Proceedings - 8th International Conference on Intelligent Networks and Intelligent Systems, ICINIS 2015*, no. 10, pp. 74–77, 2016, doi: 10.1109/ICINIS.2015.35.

[40] R. Chen and J. S. Liu, "Mixture Kalman ®lters," *J.R. Statist. Soc.B*, pp. 493–508, 2000.